Deuterium retention in chemically vapor deposited tungsten carbide coatings and hot-rolled tungsten exposed to low-energy deuterium plasma

V.Kh. Alimov[a*], J. Roth[b]

[a] Frumkin Institute of Physical Chemistry and Electrochemistry, Russian Academy of Sciences, Moscow 119071, Russia

[b] Max-Planck-Institut für Plasmaphysik, D-85748 Garching, Germany

Abstract

Chemically vapor deposited (CVD) tungsten carbides coatings $W_{45}C_{55}$ and $W_{60}C_{40}$ and hot-rolled tungsten were exposed to low-energy (about 200 eV/D) deuterium plasma with an ion flux of about 1.1×10^{21} D/m^{2}s to a fluence of about 2×10^{24} D/m^2 at sample temperatures ranging from 323 to 813 K. Trapping of deuterium was examined by the D(^{3}He,p)^{4}He nuclear reaction at ^{3}He ion energies from 0.69 to 4.0 MeV allowing the determination of the deuterium concentration at depths up to 7 μm. Based on the measured deuterium depth profiles and assuming that these profiles are determined by diffusing D atoms, the diffusion coefficients of deuterium in the CVD tungsten carbide coatings were determined. Using these diffusion coefficients, an estimate of the Arrhenius relation for the diffusion coefficients of deuterium in CVD tungsten carbide coatings was obtained: $D = 2.5\times10^{-3}\exp(-1.12\text{ eV}/kT)$ m^{2}s, where T is temperature, k is the Boltzmann constant. The concentration of trapped deuterium in the bulk of CVD tungsten carbide coatings is practically independent of the stoichiometry of the coatings. It decreases from about 5×10^{-2} to about 7×10^{-4} D/(W+C) with an increase in the deuterium plasma exposure temperature from 373 to 813 K. The concentration of trapped deuterium in hot-rolled tungsten, expressed in units of the D/W atomic ratio, is more than an order of magnitude lower than the concentration of deuterium in tungsten carbides, also decreasing with increasing plasma exposure temperature.

Keywords: CVD tungsten carbide coatings, Tungsten, Deuterium plasma exposure, Deuterium depth profiles, Deuterium diffusion coefficients

* Corresponding author

E-mail address: vkahome13@gmail.com (V.Kh. Alimov)

1. Introduction

The currently proposed DEMO divertor design consists of monoblocks made from oxide-dispersion-strengthened tungsten alloy (ODS-W) armor as plasma facing material and CuCrZr alloy as heat sink [1]. The working temperature of the ODS-W tiles is expected to be between 800 and 1200 ºC [2]. However, the service temperature of the CuCrZr alloy, chosen as heat sink material due to its high conductivity and high strength, is relatively low and ranges from 180 to 350 ºC [3], as softening and creep are observed at temperatures around 300-350 ºC. In addition, the CuCrZr alloy suffers irradiation embrittlement and can only be useful at displacement-damage levels up to around 5 dpa [4]. Since the optimum operating temperature windows for these divertor materials do not overlap, a compatible thermal barrier interlayer between the plasma facing ODS-W tiles and the CuCrZr heat sink is required to ensure a smooth thermal transition, which in addition may mitigate radiation damage in the heat sink [5]. An ideal thermal barrier material should also attenuate the energetic neutrons from the D-T reaction and absorb the gamma-rays produced by the interaction of these neutrons with tungsten and the thermal barrier material.

Tungsten carbides combine favorable properties such as high hardness, good wettability with molten metals such as copper, low thermal conductivity compared to pure tungsten, and tungsten-like thermal expansion characteristics with sufficient electrical conductivity and a high melting point [6]. In addition, tungsten carbides have a high macroscopic neutron absorption cross section, are effective neutron moderators with high moderating power, and have a high attenuation coefficient for high-energy gamma rays [7]. All these properties make tungsten carbides promising candidates for providing a thermal barrier between the plasma facing ODS-W tiles and the CuCrZr heat sink. Hydrogen isotopes from the burning plasma will penetrate the tungsten-based alloy tiles and reach the tungsten carbide thermal barrier. In this regard, it is of interest to study the behavior of hydrogen isotopes in tungsten carbides.

There are only a few works on deuterium (D) trapping in and thermal release from tungsten containing carbon, prepared by chemical vapor deposition [8, 9] or by high-temperature annealing tungsten foils in contact with carbon films [10-12]. Subsequently implanted D ions occurred at elevated energies in the range of several keV. It has been found that after irradiation with 1.5 keV D ions at room temperature, the amount of deuterium retained in chemically vapor deposited (CVD) tungsten carbide coatings $W_{85}C_{15}$ and $W_{60}C_{40}$ is more than two times that of tungsten containing no carbon atoms [8].

In the CVD tungsten carbide coatings $W_{60}C_{40}$ and $W_{85}C_{15}$ irradiated with 1.5 keV D ions at temperatures in the range from 300 to1020 K, the deuterium inventory steeply decreases with an increase in the target temperature from 300 to 550 K [8]. Thermal desorption of deuterium from the CVD tungsten carbide coatings $W_{60}C_{40}$ and $W_{85}C_{15}$ occurs at temperatures much lower than for graphite, and the TDS spectra show much more complex features. The TDS peak temperatures depend on the carbon concentration in the various phases of the tungsten carbide samples [8].

After irradiation with 5 keV D ions at room temperature, the amount of retained deuterium atoms in the near surface layer of the carbide WC foil is greater than in pure tungsten specimens. The subsequent thermal release of deuterium retained in the W foils with various carbon contents occurred rapidly at a temperature of about 350 K, while for pure tungsten, the thermal release of deuterium occurred at about 450 K [12].

Depth profiles of deuterium concentration in a CVD coating consisting of a mixture of face-centered cubic carbide WC (about 90%) and close-packed hexagonal carbide W_2C (about 10%) were studied after irradiation with 10 keV D ions at 300 and 650 K. The profiles were determined to a depth of 0.5 μm using secondary ion mass spectrometry (SIMS) and residual gas analysis (RGA) in the course of surface sputtering. D_2 molecules were not detected in the RGA measurements, so it can be concluded that deuterium is retained in the carbide matrix in the atomic state [9]. It is pertinent to note that, using first-principles calculations to study the behavior of hydrogen in hexagonal tungsten carbide WC, it was found that the binding energy between two interstitial hydrogen atoms is negative, suggesting that one hydrogen is not capable of attracting an other hydrogen atom to form a hydrogen molecule [13].

No data on hydrogen solubility and diffusivity in tungsten carbides are available.

It was previously shown that in the co-deposited deuterium-tungsten-carbon layers, the deuterium concentration is about an order of magnitude higher than the deuterium concentration in the co-deposited deuterium-tungsten layers (Ref. [14], Fig. 6 therein). From this fact, one should expect that the accumulation of hydrogen isotopes in tungsten carbides would be much higher than in pure tungsten.

The aim of this work is to determine the concentration of deuterium in CVD tungsten carbide coatings exposed to low-energy (about 200 eV/D) deuterium plasma at elevated temperatures. Exposure of tungsten carbide coatings to the low-energy deuterium plasma makes it possible to simulate the introduction of hydrogen isotopes penetrating through a tungsten-based tile during fusion plasma discharges. For comparison, in this work, we also determined the values

of the deuterium concentration in the bulk of hot-rolled tungsten (W) exposed to low-energy deuterium plasma at elevated temperatures. Preliminary results of our studies were mentioned in a compilation of hydrogen retention in ITER's plasma facing materials [15]

2. Experimental

Tungsten carbides coatings $W_{45}C_{55}$ and $W_{60}C_{40}$ were deposited on nickel substrates 10×10 mm^2 in size by chemical vapor deposition from a mixture of tungsten hexafluoride WF_6, methane, and hydrogen at temperatures of 723-823 K [16, 17], and used in this work. Depending on the deposition temperature and partial pressures of gaseous reactants in the tungsten hexafluoride–hydrogen–methane mixture, the CVD coatings of WC phase and W_2C phase, both with about 10 at.% of free carbon atoms (not chemically bounded to W atoms), were obtained. It should be noted that the surfaces of the CVD coatings consisting of the W_2C phase with about 10 at.% of free carbon atoms (hereinafter referred to as CVD $W_{60}C_{40}$ coatings) were significantly roughened; therefore, these surfaces were polished with fine-grained sandpaper. The chemical composition of the CVD coatings was determined by energy-dispersive X-ray microanalysis, and the phase composition of the coatings and the crystallite size were examined by X-ray diffractometry (Table 1) [18].

Hot-rolled tungsten with a purity of 99.95 wt.% and a grain size of 1-5 microns was also used in this work. Samples 6×8 mm^2 in size were cut from a 0.5 mm thick sheet by the spark cutting method. The surfaces of W samples were mechanically and electrochemically polished, cleaned in an ultrasonic bath with acetone, and annealed in vacuum at 1223 K for 1 h to relieve stresses arising during the polishing process.

The tungsten carbide coatings and hot-rolled tungsten samples were exposed to deuterium plasma at sample temperatures T_{exp} ranging from 323 to 813 K. The plasma was generated in a planar dc magnetron operating with D_2 gas at a pressure of about 1 Pa. The sample was placed on the magnetron cathode surface and held by a tantalum mask with an aperture of 5 mm in diameter. The sample was bombarded with plasma ions accelerated in the cathode sheath of the magnetron discharge with a discharge voltage of 450 V. For assessment of the ion energy, the spatial distribution of the plasma potential was measured using Langmuir probes. The measurement showed a cathode drop voltage of about 0.85 of the discharge voltage. Assuming that the plasma is dominated by D_2^+ ions, the mean energy per D atom was estimated to be about 200 eV [19]. The ion flux was determined from ion current measurements and was about 1.1×10^{21}

D/m^2s. All samples were exposed to the deuterium plasma for 30 min, resulting in a fluence of about 2×10^{24} D/m^2. During plasma exposure the sample temperature was controlled by a chromel–alumel thermocouple attached to the front surface of the sample outside the irradiation area.

Deuterium concentration profiles over depth were determined by nuclear reaction analysis (NRA) at the Max-Planck-Institut für Plasmaphysik, Garching. The deuterium concentration within the near-surface layer (at depths up to about 0.5 μm) was measured by means of the $D(^3He,\alpha)H$ reaction at a ^3He energy of 0.69 MeV, and the α-particles were energy-analyzed with a small-angle surface barrier detector with a solid angle of 9.16 msr at the laboratory scattering angle of 102º. The α-spectrum was transformed into a deuterium depth profile using the program SIMRNA [20].

To determine the deuterium concentration at great depths, down to 7 μm, the energy of the analyzing beam of ^3He ions was varied from 0.69 to 4.0 MeV. The protons from the $D(^3He,p)^4He$ nuclear reaction were counted using a wide-angle proton detector with a solid angle of 0.15 sr placed at a scattering angle of 135º. The $D(^3He,p)^4He$ nuclear reaction has a broad maximum at around 0.63 MeV, which can be used for resonant depth profiling. In order to determine the deuterium concentration profile in deeper layers, the computer program SIMNRA was used for the deconvolution of the proton yields measured at different ^3He ion energies. A deuterium depth distribution was assumed taking into account the near-surface depth profile obtained from the α-particle spectrum, and the proton yield as a function of incident ^3He energy was calculated. The form of the deuterium depth profile was then varied using an iterative technique until the calculated proton yield curve matched the measured proton yields [21]. The depth scales for the tungsten carbide coatings were calculated based on the following density values for stoichiometric tungsten carbides: for WC - ρ_{WC} = 15.7 g/cm^3 (atomic density $N_{WC} = 9.6\times10^{22}$ $(W+C)/cm^3$); for W_2C - ρ_{W2C} = 17.2 g/cm^3 (atomic density $N_{W2C} = 8.2\times10^{22}$ $(W+C)/cm^3$).

The surface topography of the plasma-exposed samples was examined by scanning electron microscopy (SEM).

3. Results and discussion

The deuterium depth profiles for the CVD tungsten carbide coatings and tungsten samples exposed to low-energy (about 200 eV/D) deuterium plasma to a fluence of about 2×10^{24} D/m^2 at

various temperatures, T_{ext}, are shown in Fig. 1 (for CVD tungsten carbide samples) and Fig. 2 (for hot-rolled tungsten samples).

In the CVD tungsten carbide coatings exposed to deuterium plasma at temperatures in the range from 373 to 433 K, the concentration of trapped deuterium decreases from 1-3 at.% in the near-surface layer to 0.01 at.% at a depth of about 1 μm. With an increase in the exposure temperature, the deuterium depth profiles acquire a flatter shape, falling rather sharply at the interface between the CVD coating and the nickel substrate. At the same time, the concentration of deuterium in the bulk of these tungsten carbide coatings decreases with an increase in the plasma exposure temperature (Fig. 1 a, b).

In the hot-rolled tungsten sample exposed to deuterium plasma at 323 K, the deuterium concentration decreases from about 0.5 at.% in the near-surface layer to 0.01 at.% at a depth of about 2 μm. After plasma exposures at temperatures of 418 and 493 K, the deuterium depth profiles are characterized by a near-surface concentration of 0.4-0.5 at.%, decreasing to a depth of about 0.2 μm, then a significant increase in concentration to a depth of 1-2 μm, and a further gradual decrease in concentration (Fig. 2 a). After plasma exposures in the temperature range from 573 to 783 K, the deuterium depth profiles show only near-surface peaks and plateau-like deuterium depth profiles at a depth of up to 7 μm (Fig. 2 b).

SEM images of CVD coatings $W_{45}C_{55}$, both unexposed and exposed to deuterium plasma, show the wavy surface of the samples under study (Fig. 3 a, c, e). Obviously, this wavy surface was formed during the chemical vapor deposition process. The surfaces of CVD coatings $W_{60}C_{40}$ are characterized by defects in the form of grooves, most likely caused by polishing with a fine-grained sandpaper during sample preparation (Fig. 3 b, d, f). It is important to note that SEM studies of the surfaces of CVD coatings $W_{45}C_{55}$ and $W_{60}C_{40}$, did not reveal the formation of blisters (Fig. 3).

As noted above, according to the results of first-principles calculations, in hexagonal tungsten carbide WC, a single hydrogen atom is not capable of attracting other hydrogen atom to form a hydrogen molecule [13]. Apparently, the absence of a molecular phase in the bulk of tungsten carbides can be additionally explained both by the low probability of the formation of vacancy complexes and micro-cavities in the tungsten carbide matrix under exposure with low-energy deuterium plasma, and by a small value of the hydrogen recombination coefficient on the tungsten carbide surface [22].

No blisters were observed on the surface of a hot-rolled tungsten sample exposed to deuterium plasma at 323 and 638 K (Fig. 4 a, d). However, exposure of tungsten samples to

deuterium plasma at temperatures of 418 and 493 K led to the formation of blisters on the surface (Fig. 4 b, c). If after plasma exposure at 418 K the size of the blisters ranged from 3 to 10 μm (Fig. 4 b), then after plasma exposure at 493 K the size of the blisters increased to 5–20 μm (Fig. 4 c).

The formation of blisters on the surface of a hot-rolled tungsten sample exposed to a low-energy deuterium plasma at 418 and 493 K (Fig. 4 b, c) explains the increased concentration of deuterium at a depth of 1-2 μm for the same tungsten samples (Fig. 2 a). During exposure of the tungsten sample with low-energy, high-flux deuterium plasma with ion energy well below the displacement threshold, the transient deuterium concentration in the near-surface zone greatly exceeds the solubility limit and stresses the tungsten matrix. When the compressive stress induced by the deuterium super-saturation exceeds the yield stress of the material, fracture deformation and/or plastic deformation occur [23], and intergranular/intragranular cracks (cavities) and blisters are generated [24-26]. However, with an increase in the temperature during exposure to the deuterium plasma, the solubility of deuterium, the diffusion coefficient, and the rate of surface recombination increase strongly. The transition concentration of deuterium will not exceed the solubility. In this case, hardly any blisters are observed, and the deuterium depth profiles acquire a plateau-like form (Fig. 2 b). It should be noted that the limit of the temperature of irradiation, above which blistering is not observed, shifts towards higher temperatures with an increase in the ion flux [27].

The values of the deuterium concentration in the bulk of CVD tungsten carbide coatings and hot-rolled tungsten exposed to low-energy deuterium plasma are shown in Fig. 5. The concentration of trapped deuterium in the bulk of CVD coatings $W_{45}C_{55}$ and $W_{60}C_{40}$ is practically independent of the stoichiometry of the carbide and decreases from about 5×10^{-2} to about 7×10^{-4} D/(W+C) with an increase in the deuterium plasma exposure temperature from 373 to 813 K. The concentration of trapped deuterium in hot-rolled tungsten, expressed in units of the D/W atomic ratio, is more than an order of magnitude lower than the concentration of deuterium in tungsten carbides also decreasing with increasing plasma exposure temperature.

The rather high concentration of deuterium in CVD coatings $W_{45}C_{55}$ and $W_{60}C_{40}$ is comparable to the concentration of deuterium in the carbon fiber composite NB31 [15, 28], exposed to deuterium plasma in the same setup and under the same conditions as in this work. This gives reason to believe that carbon atoms, either free or possibly bonded to tungsten atoms, are the main traps responsible for retaining deuterium in these CVD tungsten carbide coatings.

In hot-rolled tungsten, deuterium diffusing into the bulk of the material is captured by intrinsic defects, such as dislocation-type defects and vacancies at grain boundaries [29].

Based on the measured deuterium depth profiles and the assumption that these profiles are consistent with the diffusion profiles, it is possible to estimate the values of the deuterium diffusion coefficient in the tungsten carbide coatings and hot rolled tungsten samples for relatively low temperatures of deuterium plasma exposure. We assume that

(i) the transition concentration of deuterium in the near-surface zone is comparable to or exceeds the solubility limit,

(ii) the traps responsible for the accumulation of deuterium in the CVD tungsten carbide coatings, as well in the hot-rolled tungsten samples, are saturable strong traps[1] and

(iii) the concentration of traps is constant throughout the thickness of the samples.

Then the deuterium profile in these samples exposed to deuterium plasma should be consistent with saturable strong traps being filled by diffusion from the surface. Based on the measured deuterium depth profiles (Figs. 6 and 7) and assuming that these profiles are consistent with the diffusion profiles, the values of the diffusion coefficient of deuterium in CVD tungsten carbide coatings and hot-rolled W samples can be estimated. For the case of a constant deuterium concentration C_0 in the near-surface layer, which is realized upon prolonged exposure with deuterium plasma, the deuterium concentration $C(x)$ at a depth x can be described by the following Equation:

$$C(x) = C_0[1 - \mathrm{erf}(\frac{x}{2\sqrt{Dt}})], \quad (1)$$

where $\mathrm{erf}(\frac{x}{2\sqrt{Dt}})$ is the error function, D is the diffusion coefficient of deuterium, and t is the duration of exposure with deuterium plasma [31]. For each depth distribution of deuterium, the concentration C_0 and the deuterium diffusivity were varied until the profile calculated according to Eq. (1) coincided with the measured profile of deuterium (Figs. 6 and 7). It should be noted that the deuterium diffusion coefficients could not be evaluated after plasma exposure at temperatures above 543 K, since in these cases the deuterium concentration was practically constant over depth and could not be correctly described by Eq. (1). However, in these cases, the

[1] Saturable traps are traps having finite capacity. Traps where solute deuterium atom becomes trapped when it encounters unoccupied traps are denoted as strong traps [30].

concentration of C_0 was determined by the measured constant concentration of deuterium. It can be assumed that if the concentration of defects responsible for the retention of deuterium is practically constant in the bulk of the materials under study, then with prolonged exposure to deuterium plasma, the concentration of deuterium in the bulk will be practically equal to the concentration of C_0.

It should be noted that for hot-rolled tungsten exposed to deuterium plasma at a temperature of 418 K, the determination of the deuterium diffusion coefficient by matching with the error function was carried out using the deuterium profile at depths greater than 3 μm (Fig. 7). At these depths, the concentration profile is determined by the inward diffusion of deuterium and trapping in intrinsic traps. The deuterium concentration profile at depths up to 3 μm is mainly due to the accumulation of deuterium in subsurface cavities, which are visually observed in the form of blisters on the sample surface, and cannot be associated with the diffusion distribution of deuterium. It should be understood that the value of the diffusion coefficient of deuterium obtained based on the distribution profile at depths greater than 3 μm may represent the lower limit.

The evaluated values of the diffusion coefficients of deuterium in the CVD $W_{45}C_{55}$ and $W_{60}C_{40}$ coatings and hot-rolled W samples are shown in Fig. 8. The values of the diffusion coefficients of hydrogen (protium) in tungsten, taken from Frauenfelder [32] and Zakharov et al. [33], are also shown in this figure for comparison. The fact that the values of the diffusion coefficient of hydrogen measured at high temperatures [32, 33] extrapolate rather well to the values of the diffusion coefficient of deuterium in hot rolled tungsten, estimated in his work for much lower temperatures. Therefore, it is quite appropriate to assume that modeling the diffusion profiles of deuterium using Eq. (1) makes it possible to estimate the values of the diffusion coefficients for tungsten carbide coatings.

The limited number of values of the deuterium diffusion coefficient in the CVD tungsten carbide coatings does not allow an accurate determination of the values of the diffusion activation energy and the pre-exponential factor for each type of tungsten carbide coating. However, using all the data obtained in this work for the CVD tungsten carbide coatings $W_{45}C_{55}$ and $W_{60}C_{40}$ (Fig. 8), a rough estimate of the Arrhenius relation for the diffusion coefficients of deuterium in CVD tungsten carbide coatings could be obtained:

$$D = 2.5\times10^{-3} \exp(-1.12 \text{ eV}/kT) \text{ m}^2\text{s}, \quad (2)$$

where T is temperature, k is the Boltzmann constant ($k = 8.617\times10^{-5}$ eV K^{-1}).

4. Summary

The concentration of deuterium in CVD tungsten carbide coatings $W_{45}C_{55}$ and $W_{60}C_{40}$ and hot-rolled tungsten samples exposed to low-energy (about 200 eV/D) deuterium plasma at elevated temperatures was measured by the $D(^3He,p)^4He$ nuclear reaction technique. The concentration of trapped deuterium in the bulk of CVD tungsten carbide coatings is practically independent of the stoichiometry of the coatings and decreases from about 5×10^{-2} to about 7×10^{-4} D/(W+C) with an increase in the deuterium plasma exposure temperature from 373 to 813 K. The concentration of trapped deuterium in hot-rolled tungsten is more than an order of magnitude lower than the concentration of deuterium in tungsten carbides, also decreasing with increasing plasma exposure temperature.

Based on the measured deuterium depth profiles, the diffusion coefficients of deuterium in the CVD tungsten carbide coatings were determined. With the assumption that these profiles are determined by diffusing deuterium atoms which eventually get trapped in the bulk material, diffusion dominated depth profiles could be fitted to the data using the near surface concentration C_0 and the diffusion coefficient as fitting parameters. Consequently, an estimate of the Arrhenius relation for the diffusion coefficients of deuterium in the CVD tungsten carbide coatings was obtained.

The results obtained are the first data on the diffusion coefficients of deuterium and on the concentration of deuterium in CVD coatings consisting of tungsten carbides and free carbon. Additional research is required for a more detailed understanding of the behavior of hydrogen isotopes in stoichiometric tungsten carbides.

Acknowledgements

The authors are grateful to V.P. Kuzmin (Frumkin Institute of Physical Chemistry and Electrochemistry, Moscow) for the preparation of CVD tungsten carbide samples, D.A. Komarov (Frumkin Institute of Physical Chemistry and Electrochemistry, Moscow) for assistance in exposing the samples to deuterium plasma, and also J. Dorner and M. Fußeder (Max-Planck-Institut für Plasmaphysik, Garching) for technical assistance in analyzing with the ^3He beam.

References

[1] J.H. You, E. Visca, C. Bachmann, T. Barrett, F. Crescenzi, M. Fursdon, H. Greuner, D. Guilhem, P. Languille, M. Li, S. McIntosh, A.V. Müller, J. Reiser, M. Richou, M. Rieth, European DEMO divertor target: operational requirements and material-design interface, Nucl. Mater. Energy 9 (2016) 171-176 https://doi.org/10.1016/j.nme.2016.02.005

[2] M. Rieth, B. Dafferner, Limitations of W and W–1%La_2O_3 for use as structural materials, J. Nucl. Mater. 342 (2005) 20-25 https://doi.org/10.1016/j.jnucmat.2005.03.013

[3] D. Stork, P. Agostini, J.L. Boutard, D. Buckthorpe, E. Diegele, S.L. Dudarev, C. English, G. Federici, M.R. Gilbert, S. Gonzalez, A. Ibarra, C. Linsmeier, A. Li Puma, G. Marbach, P.F. Morris, L.W. Packer, B. Raj, M. Rieth, M.Q. Tran, D.J. Ward, S.J. Zinkle, Developing structural, high-heat flux and plasma facing materials for a near-term DEMO fusion power plant: the EU assessment, J. Nucl. Mater 455 (2014) 277-291 https://doi.org/10.1016/j.jnucmat.2014.06.014

[4] T.R. Barrett, G. Ellwood, G. Perez, M. Kovari, M. Fursdon, F. Domptail, S. Kirk, S.C. McIntosh, S. Roberts, S. Zheng, L.V. Boccaccini, J.-H. You, C. Bachmann, J. Reiser, M. Rieth, E. Visca, G. Mazzone, F. Arbeiter, P.K. Domalapally, Progress in the engineering design and assessment of the European DEMO first wall and divertor plasma facing components, Fusion Eng. Des. 109-111 (2016) 917-924 https://doi.org/10.1016/j.fusengdes.2016.01.052

[5] E. Tejado, M. Dias, J.B. Correia, T. Palacios, P.A. Carvalho, E. Alves, J.Y. Pastor, New WC-Cu thermal barriers for fusion applications: High temperature mechanical behaviour, J. Nucl. Mater. 498 (2018) 355-361 https://doi.org/10.1016/j.jnucmat.2017.10.071

[6] M. Dias, F. Guerreiro, E. Tejado, J.B. Correia, U.V. Mardolcar, M. Coelho, T. Palacios, J.Y. Pastor, P.A. Carvalho, E. Alves, WC-Cu thermal barriers for fusion applications, Surf. Coating. Technol. 355 (2018) 222-226 https://doi.org/10.1016/j.surfcoat.2018.02.086

[7] S.X. Oliver, M.L. Jackson, P.A. Burr, Radiation-induced evolution of tungsten carbide in fusion reactors: accommodation of defect clusters and transmutation elements, ACS Appl. Energy Mater. 3 (2020) 868−878 https://doi.org/10.1021/acsaem.9b01990

[8] W. Wang, V.Kh. Alimov, B.M.U. Scherzer, J. Roth, Deuterium trapping in and release from tungsten carbide, J. Nucl. Mater. 241-243 (1997) 1087-1092 https://doi.org/10.1016/S0022-3115(97)80199-7

[9] V.Kh. Alimov, Deuterium retention in pure and mixed plasma facing materials, Phys. Scr. T 108 (2004) 46-56 https://doi.org/10.1238/Physica.Topical.108a00046

[10] T. Horikawa, B. Tsuchiya, K. Morita, Retention and re-emission of deuterium implanted into tungsten monocarbide, J. Nucl. Mater. 258-263 (1998) 1087-1091 https://doi.org/10.1016/S0022-3115(98)00279-7

[11] T. Horikawa, B. Tsuchiya, K. Morita, Dynamic behavior of hydrogen isotopes in tungsten-carbon composite materials, J. Nucl. Mater. 266-269 (1999) 1091-1096 https://doi.org/10.1016/S0022-3115(98)00518-2

[12] S. Nagata, K. Takahiro, S. Horiike, S. Yamaguchi, Retention and release of deuterium implanted in W and Mo, J. Nucl. Mater. 266-269 (1999) 1151-1156 https://doi.org/10.1016/S0022-3115(98)00520-0

[13] X.-S. Kong, Y.-W. You, C.S. Liu, Q.F Fang, J.-L. Chen, G.-N. Luo, First principles study of hydrogen behaviors in hexagonal tungsten carbide, J. Nucl. Mater. 418 (2011) 233-238 https://doi.org/10.1016/j.jnucmat.2011.07.004

[14] J. Roth, E. Tsitrone, A. Loarte, Th. Loarer, G. Counsell, R. Neu, V. Philipps, S. Brezinsek, M. Lehnen, P. Coad, Ch. Grisolia, K. Schmid, K. Krieger, A. Kallenbach, B. Lipschultz, R. Doerner, R. Causey, V. Alimov, W. Shu, O. Ogorodnikova, A. Kirschner, G. Federici, A. Kukushkin, EFDA PWI Task Force, ITER PWI Team, Fusion for Energy, ITPA SOL/DIV, Recent analysis of key plasma wall interactions issues for ITER, J. Nucl. Mater. 390-391 (2009) 1-9 https://doi.org/10.1016/j.jnucmat.2009.01.037

[15] C.H. Skinner, A.A. Haasz, V.Kh. Alimov, N. Bekris, R.A. Causey, R.E.H. Clark, J.P. Coad, J.W. Davis, R.P. Doerner, M. Mayer, A. Pisarev, J. Roth, T. Tanabe, Recent advances on hydrogen retention in ITER's plasma-facing materials: beryllium, carbon, and tungsten, Fusion Sci. Technol. 54 (2008) 891-945 https://doi.org/10.13182/FST54-891

[16] A.I. Krasovsky, R.K. Chuzhko, V.R. Tregulov, O.A. Balakhovsky, Synthesis of Tungsten Carbides, in: Fluoride Process for Producing Tungsten. Physical and Chemical Foundations. Metal Properties, Nauka, Moscow, 1981, pp. 219-256 (in Russian)

[17] V.L. Goncharov, Yu.V. Lakhotkin, V.P. Kuzmin V.Kh. Alimov, J. Roth, Chemical vapor crystallization of hard nanocomposite tungsten carbide layers for extreme applications, Adv. Mater. Res. 59 (2009) 62-65 https://doi.org/10.4028/www.scientific.net/AMR.59.62

[18] V.Kh. Alimov, V.L. Goncharov, D.A. Komarov, Yu.V. Lakhotkin, V.P. Kuzmin, J. Dorner, J. Roth, Deuterim retention in CVD tungsten carbides at ion irradiation, Problems of Atomic Science and Technology, Ser. Thermonuclear Fusion, 2008, Issue 4, pp. 31-36 (in Russian)

[19] V.Kh. Alimov, J. Roth, R.A. Causey, D.A. Komarov, Ch. Linsmeier, A. Wiltner, F. Koch, S. Lindig, Deuterium retention in tungsten exposed to low-energy, high-flux clean and carbon-seeded deuterium plasmas, J. Nucl. Mater. 375 (2008) 192-201 https://doi.org/10.1016/j.jnucmat.2008.01.008

[20] M. Mayer, SIMNRA User's Guide, IPP Report IPP 9/113, Max-Planck-Institut für Plasmaphysik, Garching, 1997 home.mpcdf.mpg.de/~mam/

[21] V.Kh. Alimov, M. Mayer, J. Roth, Differential cross-section of the D (^{3}He,p) ^{4}He nuclear reaction and depth profiling of deuterium up to large depths, Nucl. Instrum. Methods Phys. Res. B 234 (2005) 169–175 https://doi.org/10.1016/j.nimb.2005.01.009

[22] O.V. Ogorodnikova, J. Roth, M. Mayer, Deuterium retention in tungsten in dependence of the surface conditions, J. Nucl. Mater. 313-316 (2003) 469-477 https://doi.org/10.1016/S0022-3115(02)01375-2

[23] J.B. Condon, T. Schober, Hydrogen bubbles in metals, J. Nucl. Mater. 207 (1993) 1-24 https://doi.org/10.1016/0022-3115(93)90244-S

[24] S. Lindig, M. Balden, V.Kh. Alimov, T. Yamanishi,W.M. Shu, J. Roth, Subsurface morphology changes due to deuterium bombardment of tungsten, Phys. Scr. T138 (2009) 014040 (5pp) https://doi.org/10.1088/0031-8949/2009/T138/014040

[25] S. Lindig, M. Balden, V.Kh. Alimov, A. Manhard, C. Höschen, T. Höschen, B. Tyburska-Püschel, J. Roth, Sub-surface structures of ITER-gradeW (Japan) and re-crystallized W after ITER-similar low-energy and high-flux D plasma loadings, Phys. Scr. T145 (2011) 014039 (7pp) https://doi.org/10.1088/0031-8949/2011/T145/014039

[26] M. Balden, S. Lindig, A. Manhard, J.-H. You, D_2 gas-filled blisters on deuterium-bombarded tungsten, J. Nucl. Mater. 414 (2011) 69-72 https://doi.org/10.1016/j.jnucmat.2011.04.031

[27] H.Y. Xu, W. Liu, G.N. Luo, Y. Yuan, Y.Z. Jia, B.Q. Fu, G. De Temmerman, Blistering on tungsten surface exposed to high flux deuterium plasma, J. Nucl. Mater. 471 (2016) 51-58 http://dx.doi.org/10.1016/j.jnucmat.2015.12.025

[28] V.Kh. Alimov, J. Roth, Hydrogen isotope retention in plasma-facing materials: review of recent experimental results, Phys. Scr. T128 (2007) 6-13 https://doi.org/10.1088/0031-8949/2007/T128/002

[29] A. Manhard, K. Schmid, M. Balden, W. Jacob, Influence of the microstructure on the deuterium retention in tungsten, J. Nucl. Mater. 415 (2011) S632-S635 https://doi.org/10.1016/j.jnucmat.2010.10.045

[30] W.R. Wampler, R.P. Doerner, The influence of displacement damage on deuterium retention in tungsten exposed to plasma, Nucl. Fusion 49 (2009) 115023 (9pp) https://doi.org/10.1088/0029-5515/49/11/115023

[31] J. Crank, Mathematics of Diffusion, University Press, Oxford, 1956

[32] R. Frauenfelder, Solution and diffusion of hydrogen in tungsten, J. Vac. Sci. Technol. 6 (1969) 388-397 https://doi.org/10.1116/1.1492699

[33] A.P. Zakharov, V.M. Sharapov, E.I. Evko, Hydrogen permeability of polycrystalline and monocrystalline molybdenum and tungsten, Sov. Mater. Sci. 9 (1975) 149-153 https://doi.org/10.1007/BF00715727

Table 1. Chemical composition and structure of CVD tungsten carbide coatings $W_{45}C_{55}$ and $W_{60}C_{40}$ [18].

	$W_{45}C_{55}$	$W_{60}C_{40}$
Chemical composition	W – 45 at.%; C – 55 at.%	W – 60 at.%; C – 40 at.%
Phase composition	fcc WC – about 90 at.%; C atoms – about 10 at.%	hcp W_2C – about 90 at.%; C atoms – about 10 at.%
Crystallite size	10-30 nm	20-30 nm
Coating thickness	3-4 μm	3-4 μm

Note: hcp - hexagonal close-packed; fcc - face-centered cubic

Figure captions

Figure 1. Depth profiles of deuterium trapped in CVD tungsten carbide coatings $W_{45}C_{55}$ (a) and $W_{60}C_{40}$ (b) exposed to low-energy (about 200 eV/D) deuterium plasma to a fluence of about 2×10^{24} D/m^2 at various temperatures

Figure 2. Depth profiles of deuterium trapped in hot-rolled W samples exposed to low-energy (about 200 eV/D) deuterium plasma to a fluence of about 2×10^{24} D/m^2 at temperatures in the range from 323 to 493 K (a) and in the range from 573 to 783 K (b). Please note that the scales of the ordinate axes on panels (a) and (b) are different.

Figure 3. SEM images of surfaces of CVD $W_{45}C_{55}$ coatings (a, c, e) and CVD $W_{60}C_{40}$ coatings (b, d, f), not exposed to deuterium plasma (a, b), and exposed to low-energy (about 200 eV/D) deuterium plasma to a fluence of about 2×10^{24} D/m^2 at various temperatures (c, d, e, f). The temperature of exposure with deuterium plasma, T_{exp}, is indicated on each of the panels (c, d, e, and f). The scale bar given in panel (f) is valid for all images. The surfaces were tilted by 70º.

Figure 4. SEM images of surfaces of hot-rolled tungsten samples exposed to low-energy (about 200 eV/D) deuterium plasma to a fluence of about 2×10^{24} D/m^2 at 323 K (a), 418 K (b), 493 K (c), and 638 K (d). The scale bar given in panel (a) is valid for all images. The surfaces were tilted by 45º.

Figure 5. Deuterium concentration in the bulk of CVD tungsten carbide coatings and hot-rolled tungsten samples exposed to low-energy (about 200 eV/D) deuterium plasma to a fluence of about 2×10^{24} D/m^2, as a function of the exposure temperature.

Figure 6. Measured (symbols) and calculated in accordance with Eq. (1) (solid lines) depth distributions of deuterium concentration in CVD tungsten carbide coatings $W_{45}C_{55}$ (a) and $W_{60}C_{40}$ (b) exposed to low-energy (about 200 eV/D) deuterium plasma to a fluence of about 2×10^{24} D/m^2 at various temperatures.

Figure 7. Measured (symbols) and calculated in accordance with Eq. (1) (solid lines) depth distributions of deuterium concentration in hot-rolled tungsten samples exposed to low-energy

(about 200 eV/D) deuterium plasma to a fluence of about 2×10^{24} D/m^2 at temperatures of 323 and 418 K.

Figure 8. Comparison of the Arrhenius relations for the diffusion coefficients of deuterium in CVD tungsten carbide coatings $W_{45}C_{55}$ and $W_{60}C_{40}$, as well as in hot-rolled tungsten samples, estimated in this work. In addition, the data on the diffusion of hydrogen (protium) in tungsten, taken from Frauenfelder [32] and Zakharov at al. [33], are also plotted.

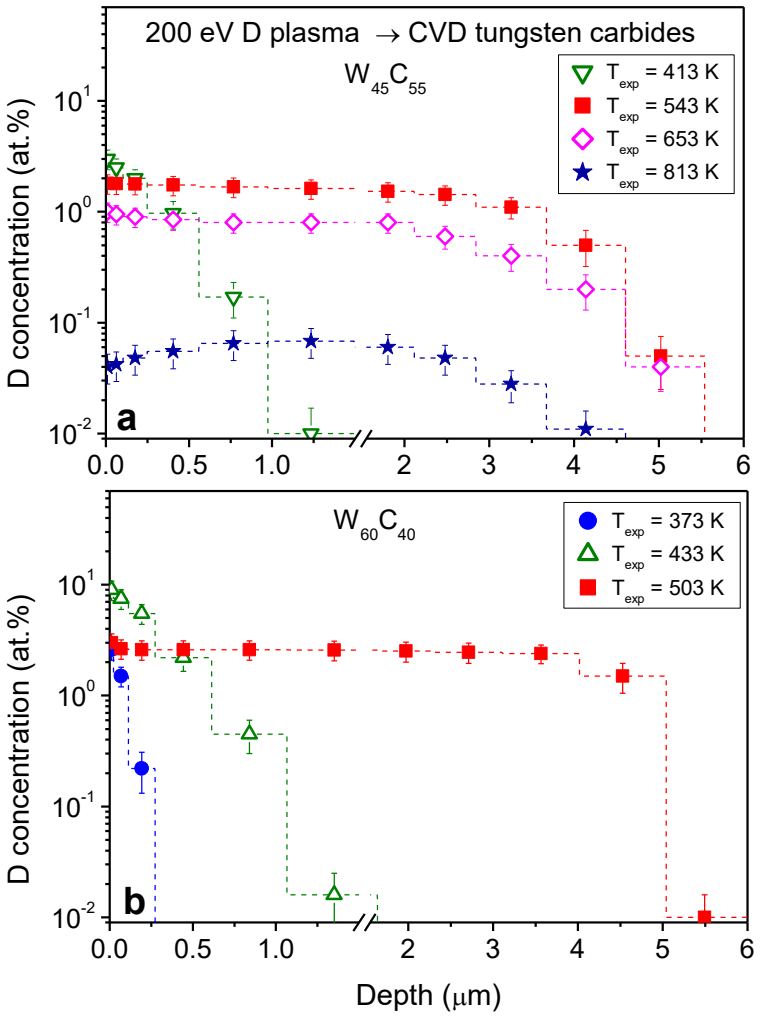

Figure 1. Depth profiles of deuterium trapped in CVD tungsten carbide coatings $W_{45}C_{55}$ (a) and $W_{60}C_{40}$ (b) exposed to low-energy (about 200 eV/D) deuterium plasma to a fluence of about 2×10^{24} D/m^2 at various temperatures

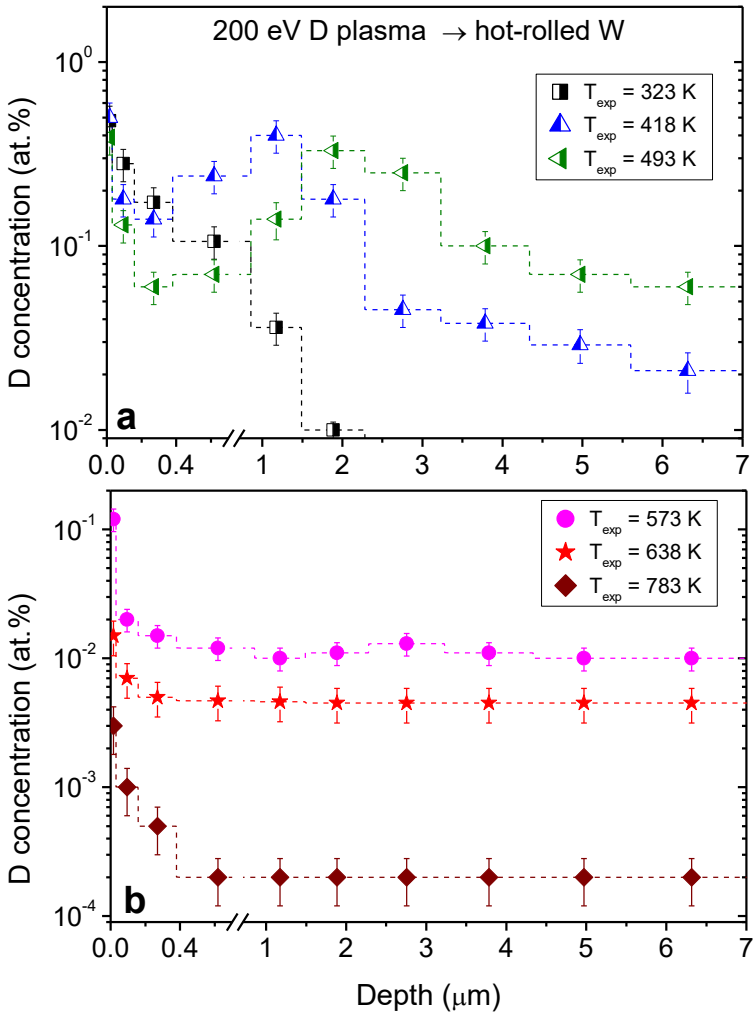

Figure 2. Depth profiles of deuterium trapped in hot-rolled W samples exposed to low-energy (about 200 eV/D) deuterium plasma to a fluence of about 2×10^{24} D/m^2 at temperatures in the range from 323 to 493 K (a) and in the range from 573 to 783 K (b). Please note that the scales of the ordinate axes on panels (a) and (b) are different.

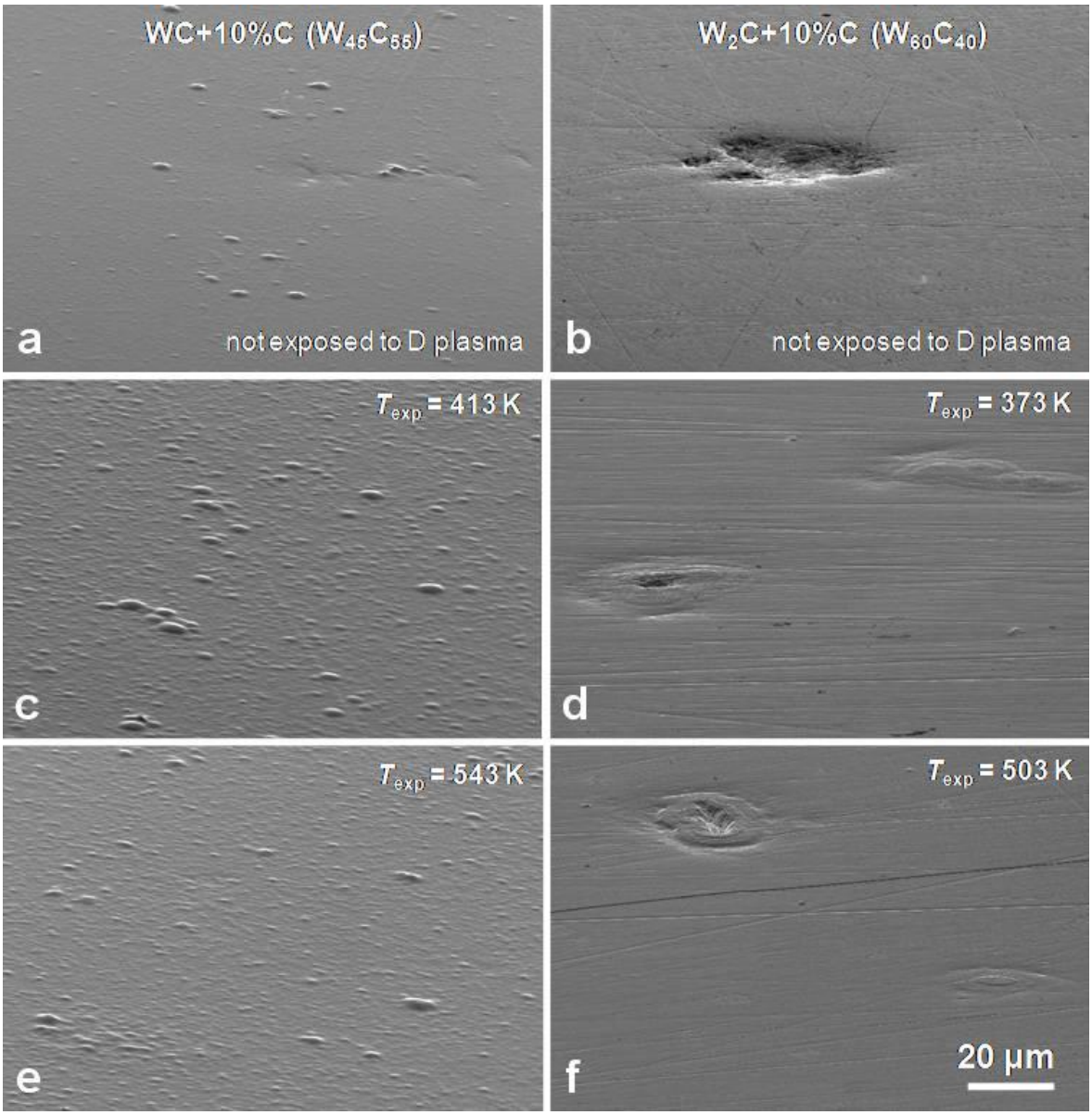

Figure 3. SEM images of surfaces of CVD $W_{45}C_{55}$ coatings (a, c, e) and CVD $W_{60}C_{40}$ coatings (b, d, f), not exposed to deuterium plasma (a, b), and exposed to low-energy (about 200 eV/D) deuterium plasma to a fluence of about 2×10^{24} D/m^2 at various temperatures (c, d, e, f). The temperature of exposure with deuterium plasma, T_{exp} , is indicated on each of the panels (c, d, e, f). The scale bar given in panel (f) is valid for all images. The surfaces were tilted by 70º.

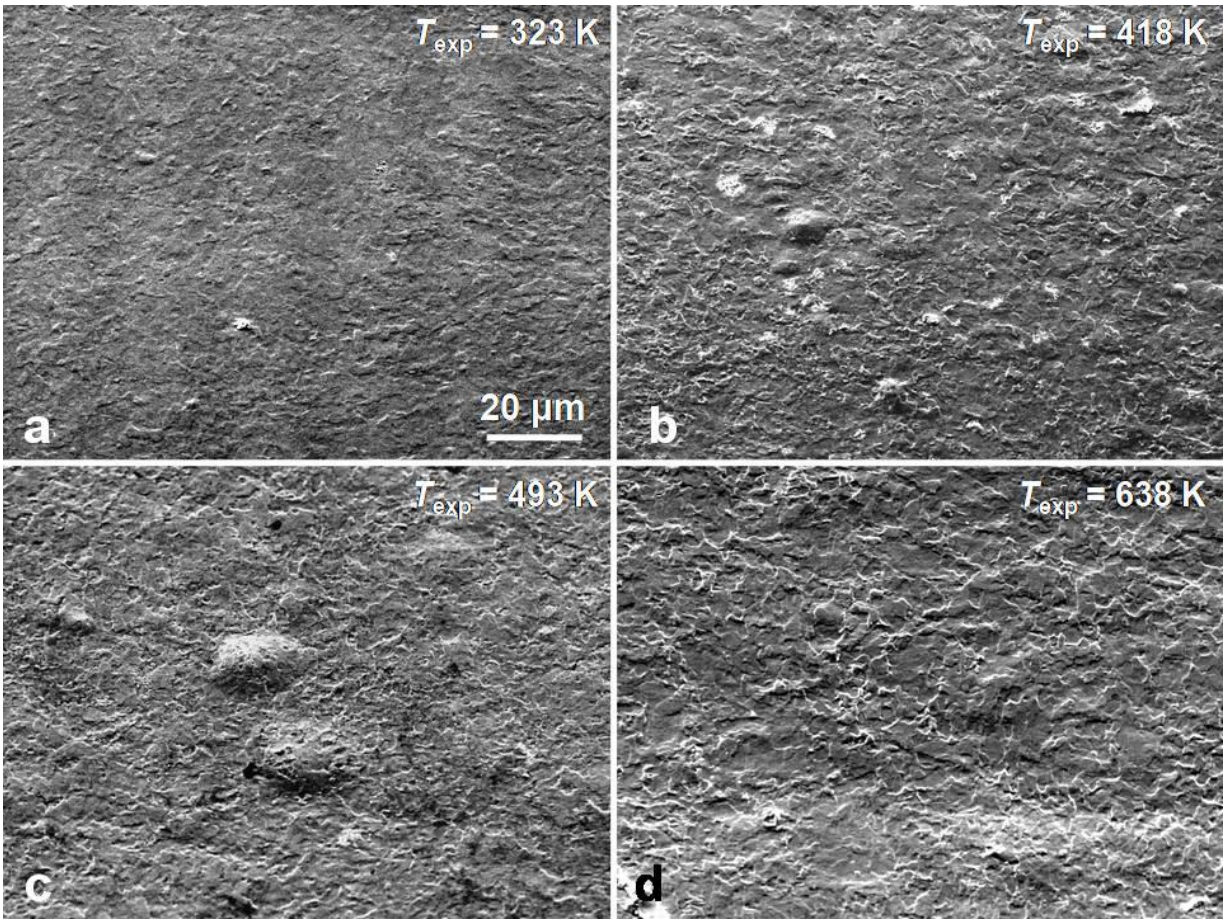

Figure 4. SEM images of surfaces of hot-rolled tungsten samples exposed to low-energy (about 200 eV/D) deuterium plasma to a fluence of about 2×10^{24} D/m^2 at 323 K (a), 418 K (b), 493 K (c), and 638 K (d). The scale bar given in panel (a) is valid for all images. The surfaces were tilted by 45º.

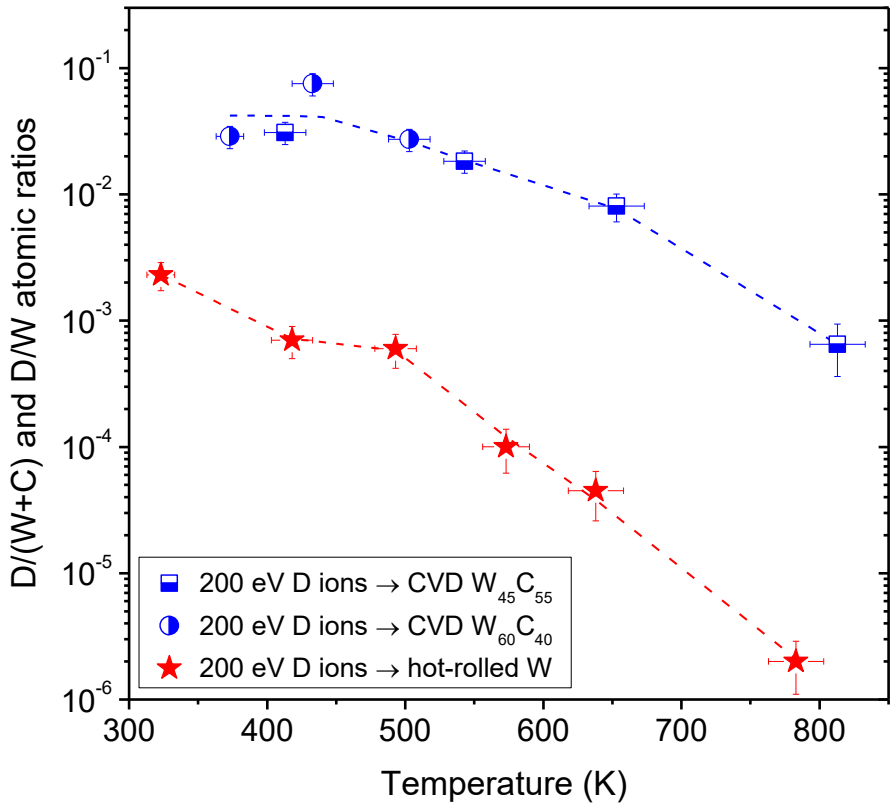

Figure 5. Deuterium concentration in the bulk of CVD tungsten carbide coatings and hot-rolled tungsten samples exposed to low-energy (about 200 eV/D) deuterium plasma to a fluence of about 2×10^{24} D/m^2, as a function of the exposure temperature.

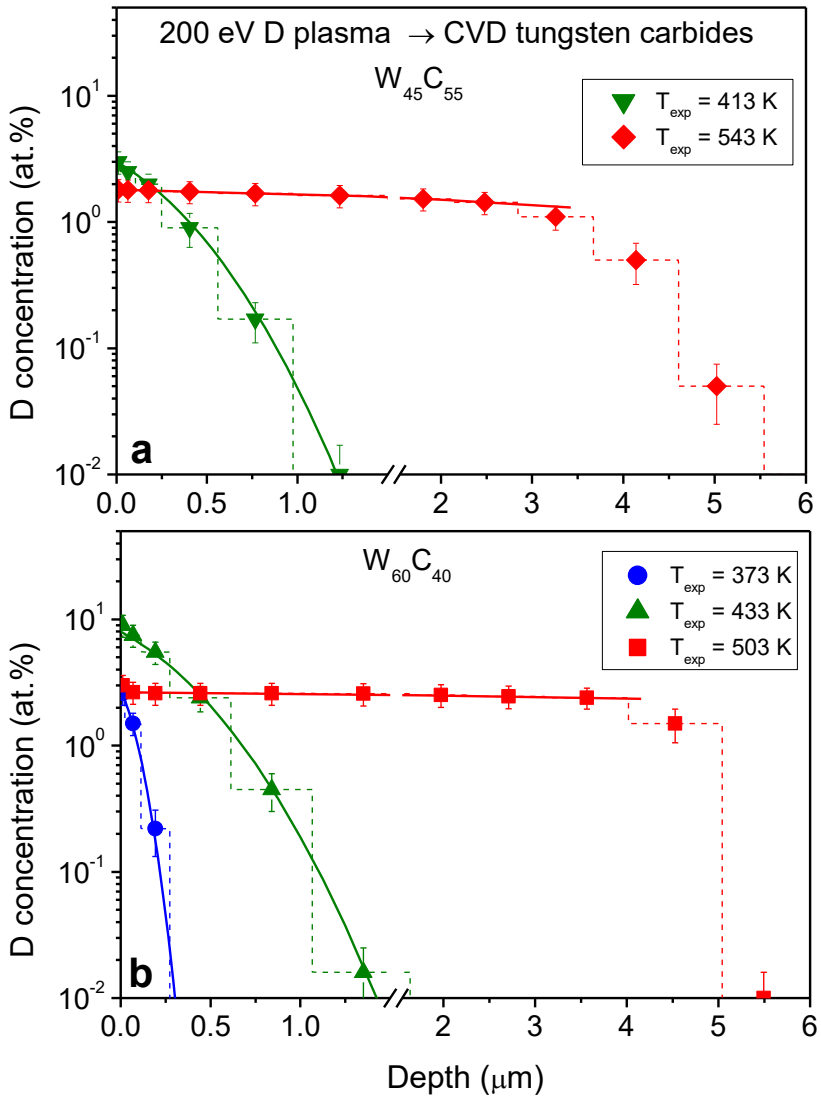

Figure 6. Measured (symbols) and calculated in accordance with Eq. (1) (solid lines) depth distributions of deuterium concentration in CVD tungsten carbide coatings $W_{45}C_{55}$ (a) and $W_{60}C_{40}$ (b) exposed to low-energy (about 200 eV/D) deuterium plasma to a fluence of about 2×10^{24} D/m^2 at various temperatures.

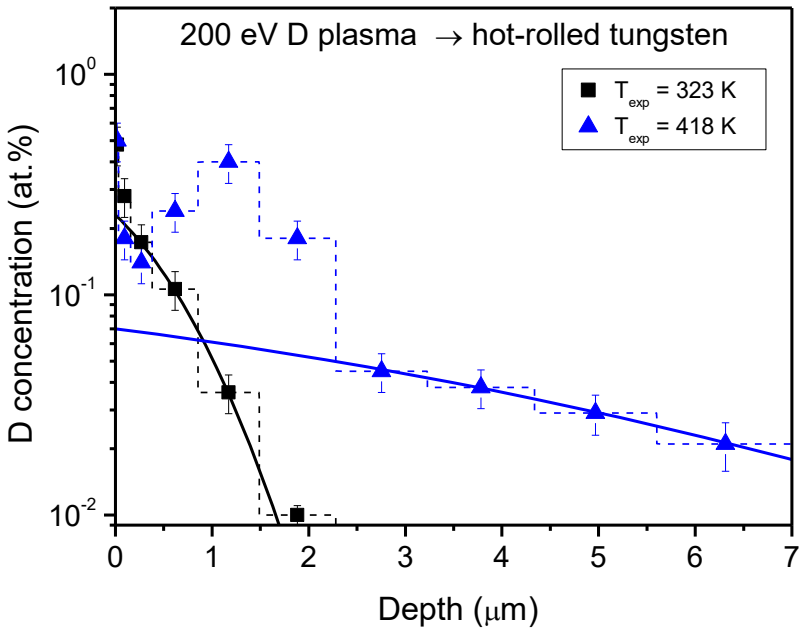

Figure 7. Measured (symbols) and calculated in accordance with Eq. (1) (solid lines) depth distributions of deuterium concentration in hot-rolled tungsten samples exposed to low-energy (about 200 eV/D) deuterium plasma to a fluence of about 2×10^{24} D/m^2 at temperatures of 323 and 418 K.

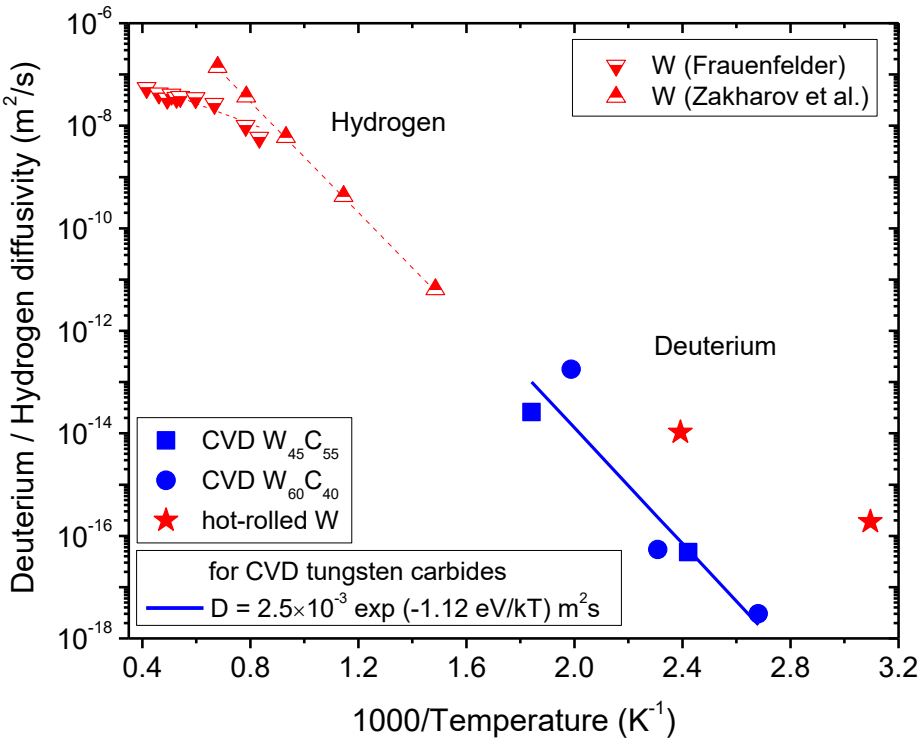

Figure 8. Comparison of the Arrhenius relations for the diffusion coefficients of deuterium in CVD tungsten carbide coatings $W_{45}C_{55}$ and $W_{60}C_{40}$, as well as in hot-rolled tungsten samples, estimated in this work. In addition, the data on the diffusion of hydrogen (protium) in tungsten, taken from Frauenfelder [32] and Zakharov at al. [33], are also plotted.